ELSEVIER

Journal of Luminescence 71 (1997) 65–70

JOURNAL OF LUMINESCENCE

Optical and scintillation properties of Ce^{3+} doped $LiYF_4$ and $LiLuF_4$ crystals

C.M. Combes[a,*], P. Dorenbos[a], C.W.E. van Eijk[a], C. Pedrini[b], H.W. Den Hartog[c], J.Y. Gesland[d], P.A. Rodnyi[e]

[a] *Radiation Technology Group, Faculty of Applied Physics, Delft University of Technology, c/o IRI, Mekelweg 15, 2629 JB Delft, The Netherlands*
[b] *Université Lyon 1, 69622 Villeurbanne Cedex, France*
[c] *University of Groningen, Groningen, The Netherlands*
[d] *Université du Maine, 72017 Le Mans Cedex, France*
[e] *State Technical University, St Petersburg, Russian Federation*

Received 26 January 1996; revised 12 August 1996; accepted 5 September 1996

Abstract

Optical properties of $LiYF_4:Ce$ and $LiLuF_4:Ce$ were studied viz. optical absorption spectra and X-ray induced emission spectra. The scintillation characteristics of $LiYF_4:Ce$ and $LiLuF_4:Ce$ were investigated viz. γ-ray induced pulse height spectra and decay time measurements. A model is presented to describe the variation of X-ray induced emission intensity of $LiYF_4:Ce$ crystals with temperature.

Keywords: Scintillation; 5d–4f luminescence; Cerium; $LiYF_4:Ce$; $LiLuF_4:Ce$

1. Introduction

Since 1960, numerous results concerning crystal growth and optical properties of $LiMF_4$, where M = Y or Lu have been reported. Several pure crystals [1–3], Ce-doped [4–7], Pr-doped [2, 3, 8–10], Nd-doped [3, 11], Ho-doped [11], Er-doped [2, 3], Tm-doped [3], or Ce–Tb co-doped crystals [12] have been studied. The strong interest in these compounds is due to their potential application as laser and lamp phosphor materials. However, lithium-containing compounds also possess the ability to convert incident neutrons into secondary ionizing particles via the reaction: ${}^{6}_{3}Li + {}^{1}_{0}n \rightarrow {}^{3}_{1}H + \alpha$ with a Q-value of 4.78 MeV. Therefore, lithium-containing compounds could provide a neutron scintillation detector. This type of application was already envisaged by Spowart [6] who compared the pulse height spectrum of a $LiYF_4:Ce$ crystal with that of a lithium-containing glass, using an Am/Be neutron source. Our interest is to study in more detail if $LiYF_4:Ce$ or $LiLuF_4:Ce$ can be used in an efficient thermal neutron scintillation detector.

$LiYF_4$ and $LiLuF_4$ have both a tetragonal scheelite structure with four formula units in the unit cell (for $LiYF_4$: $a_0 = 5.26$ Å, $c_0 = 10.94$ Å [13]; for $LiLuF_4$: $a_0 = 5.13$ Å, $c_0 = 10.55$ Å [14]) and space group $I4_1/a$. The effective ionic radii of Y^{3+} and Lu^{3+} are 1.019 and 0.977 Å, respectively [15]. The Ce^{3+} ion has only one electron in its 4f shell, and has a

* Corresponding author.

PII S0022-2313(96)00118-4

larger radius of 1.143 Å than the Y^{3+} and Lu^{3+} ions which it substitutes. The optical properties of Ce^{3+} in $LiYF_4$ and $LiLuF_4$ host crystals are very similar because of the almost identical crystal structures. The densities of $LiYF_4$ and $LiLuF_4$ are 3.97 and 5.96 g/cm^3, respectively.

2. Experimental procedure

The different crystals studied were grown, either by the Czochralski technique or the Stockbarger–Bridgman technique. The crystals were ground and polished to a thickness between ~ 1 and 5 mm with two plane-parallel faces.

The optical absorption spectra were measured with a diode array spectrophotometer (HP8452A) for a wavelength range from 200 to 800 nm. For a wavelength range from 150 to 300 nm, a deuterium lamp and vacuum ultraviolet (VUV) equipment were used. X-ray induced emission spectra were recorded between 120 and 540 nm and corrected for the transmittance of the monochromator and the quantum efficiency of the photomultiplier tube (PMT). The emission spectra were compared with the one of a pure BaF_2 crystal recorded under identical experimental conditions. Because this crystal has a well-determined light yield of about 11000 photons/MeV of absorbed X-ray energy, the absolute light output of $LiYF_4$: Ce and $LiLuF_4$: Ce, under continuous X-ray irradiation, was obtained. Pulse height spectra were recorded employing a ^{137}Cs source and an electronic shaping time of 1 μs. The absolute photon yield, in photons/MeV of absorbed γ-ray energy, was obtained by comparing the location of the 662 keV photo-peak in the pulse height spectra with the location of the maximum in the pulse height spectrum of single photoelectrons from the photocathode of the PMT. Under continuous X-ray excitation, all scintillation decay components, including afterglow, contribute to the obtained light yield whereas with γ-ray excitation the light yield depends on the electronic shaping time. Details about the experimental set-ups are described elsewhere [16]. The scintillation decay time measurements were performed by the single photon counting technique.

3. Results and discussion

The optical absorption spectrum of each crystal studied exhibits five well-defined bands at 186, 196, 206, 244 and 292 nm due to 4f–5d transitions in Ce^{3+}, see Fig. 1. The nominal Ce^{3+} concentrations are shown in Table 1. The actual Ce^{3+} concentration of one $LiYF_4$: Ce crystal and of the $LiLuF_4$: Ce crystal, was determined by the method of mass spectroscopy in solution. By comparing the absorption coefficient at 244 nm ($\mu_{244\,nm}$) of each $LiYF_4$: Ce crystal, with unknown Ce^{3+} concentration, with that of the crystal for which the Ce^{3+} concentration is known, the actual Ce^{3+} concentration was deduced, see Table 1. The error in $\mu_{244\,nm}$ is estimated to be 5%. From now on the actual Ce^{3+} concentrations are used.

A calculation of the position of the 4f and 5d energy levels of Ce^{3+} in $LiYF_4$ and $LiLuF_4$ was done by Andriessen et al. [5]. Due to the crystal-field interaction, the 5d state splits into four levels as a result of the S4 point symmetry at the Ce^{3+} site in $LiYF_4$ and $LiLuF_4$. Moreover, the spin–orbit interaction splits the level at 201 nm, which is degenerate, into two slightly separated levels. Since the energy difference between the two bands at 196 and 206 nm is much larger than the energy difference calculated from the spin–orbit interaction of the level at 201 nm, it was envisaged in [5] that there is a distortion in the S4 symmetry of Ce^{3+} in $LiYF_4$.

X-ray induced emission spectra, of both $LiYF_4$: Ce and $LiLuF_4$: Ce crystals, at room temperature, exhibit Ce^{3+} emission bands at 305 and 325 nm caused

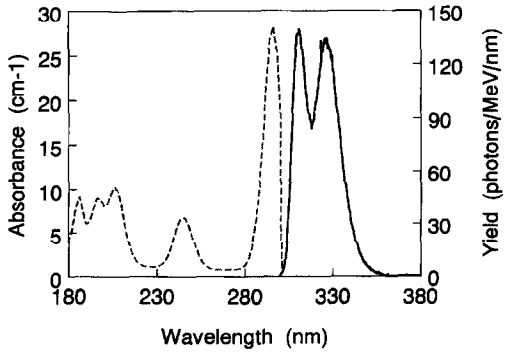

Fig. 1. X-ray induced emission spectrum and optical absorption (dashed line) spectrum of $LiLuF_4$: 0.1 mol%Ce at room temperature.

Table 1
X-ray and γ-ray induced photon yields in photons/MeV measured at room temperature, nominal Ce^{3+} concentration (mol% Ce^{3+}), absorption coefficient $\mu_{244\,nm}$ (cm^{-1}) and actual Ce^{3+} concentration (mol% Ce^{3+}) for the different Ce doped $LiYF_4$ and Ce-doped $LiLuF_4$ crystals studied

Crystal	Yield (photons/MeV) X-rays	Yield (photons/MeV) γ-rays ^{137}Cs	Nom. conc. mol% Ce^{3+}	$\mu_{244\,nm}$ (cm^{-1})	Act. conc. mol% Ce^{3+}
$LiYF_4$: Ce	3730	890	1.08	46.42	0.25
	6320	740	1.0	33.57	≥0.18
	6260	620	1.0	22.27	0.12
	6090	930	1.0	18.44	0.10[b]
	5790	1210	1.0	18.83	0.10
	2180	n.m.[a]	0.1	4.84	0.03
	2960	n.m.[a]	0.3	4.56	0.02
$LiLuF_4$: Ce	3780	n.m.[a]	1.0	15.52	0.10[b]

[a] *n.m.* means not measurable due to a very poor photopeak resolution.
[b] Concentrations which were determined by the method of mass spectroscopy in solution.

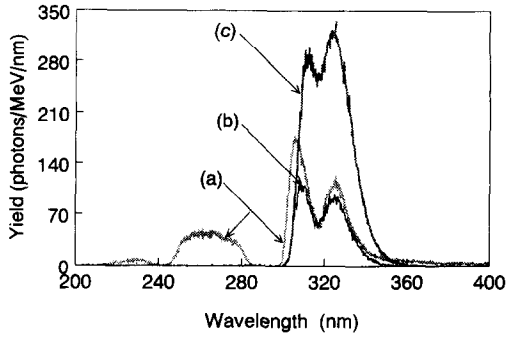

Fig. 2. X-ray induced emission spectrum of $LiYF_4$: 0.1 mol%Ce recorded at (a) T = 108 K, (b) 260 K and (c) 380 K.

by transitions from the lowest 5d level to the $^2F_{5/2}$ and $^2F_{7/2}$ levels of the $4f^1$ configuration, see Figs. 1 and 2. The photon yields obtained experimentally for the different crystals studied are presented in Table 1. In Fig. 2, X-ray induced emission spectra recorded at 108, 260 and 380 K for a crystal of $LiYF_4$: 0.1 mol%Ce are shown. The luminescence observed at low-temperature between 210 and 290 nm is attributed to self-trapped exciton (STE) emission. Hayes et al. [1] have observed a broad STE emission band between 210 and 450 nm at 4.2 K in a pure $LiYF_4$ crystal. In our case, the spectral shape of STE emission in $LiYF_4$: Ce is modified due to the presence of two Ce^{3+}-absorption bands at 244 and 292 nm, see Fig. 1, absorbing the STE emission. In Fig. 3, the variation of STE emission intensity, between 200 and 300 nm, and Ce-luminescence

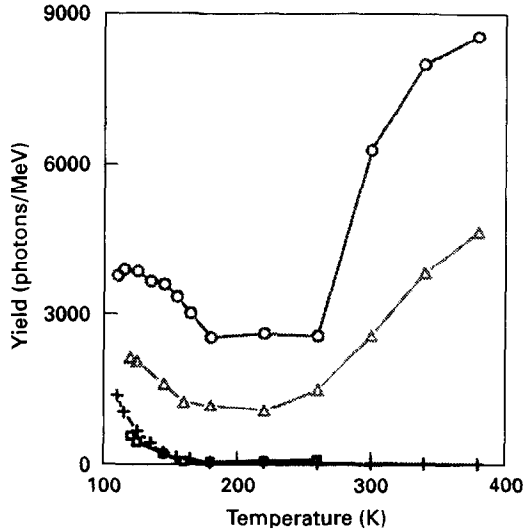

Fig. 3. Variation of STE emission and Ce-luminescence with temperature (K) for $LiYF_4$: 0.02 mol%Ce (□: STE and △: Ce) and $LiYF_4$: 0.1 mol%Ce (+: STE and ○: Ce).

intensity, between 300 and 370 nm, with temperature for $LiYF_4$: 0.02 mol%Ce and $LiYF_4$: 0.1 mol%Ce is presented. For both crystals a similar behaviour is observed. If the temperature increases from 110 to 160 K, both the STE emission and the Ce-luminescence intensities decrease. Above 160 K, the STE emission is absent and Ce-luminescence intensity is approximately constant until 220–250 K, above which the Ce-luminescence intensity increases by raising the temperature up to $T \sim 380$ K.

Table 1 presents the photon yields derived from the γ-ray induced pulse height spectra. The factor of 4–10 difference, between the light yields derived from X-ray and γ-ray excitation experiments, indicates that the scintillation decay is dominated by components much longer than the employed 1 μs shaping time. Fig. 4 shows the fast decay component of $LiYF_4$: 0.1 mol%Ce recorded at room temperature. The needle like peak appearing in the first 5 ns of the spectrum is due to an experimental artifact. A decay time of $\sim$100 ns was measured for the two $LiYF_4$: 0.1 mol% Ce crystals, and a faster decay time of $\sim$65 ns was found for the crystal doped with more than 0.18 mol%Ce. Ehrlich et al. [4] observed a decay time of $\sim$40 ns by optically exciting the second 5d level of Ce^{3+}. The difference in the decay times obtained with the two different excitation methods must be due to a more or less slow transfer of the holes and/or the electrons to the Ce ions, probably because of temporary trapping at shallow traps. The decay process is dominated by a slow component with a decay in the ms range, which could be observed using a LeCroy LS140 digital oscilloscope.

A model to describe the variations of STE emission intensity and Ce-luminescence intensity with temperature is proposed. Upon the absorption of ionizing radiation in the crystal N_{eh} electron–hole pairs are created. Eq. (1) gives the relation between the three hole-trapping possibilities. $f_{h\to F_2^-}$ represents the fraction of the holes trapped by the lattice itself and which form F_2^- centres. Another fraction $f_{h\to Ce}$ of the holes created can be directly trapped by Ce ions which gives Ce-luminescence with an assumed quantum efficiency of 100%. Also a fraction $f_{h\to K}$ of the holes are lost by non-radiative e–h recombination mechanisms.

$$f_{h\to F_2^-} + f_{h\to Ce} + f_{h\to K} = 1, \tag{1}$$

where the fractions $f_{h\to F_2^-}$, $f_{h\to Ce}$ and $f_{h\to K}$ are only Ce-concentration dependent.

Eq. (2) gives the relation between the three F_2^--trapping possibilities. A fraction $f_{F_2^-\to STE}$ of the F_2^- centres can trap electrons and form STEs. Alternatively, a fraction $f_{F_2^-\to Ce}$ of the F_2^- centres can be trapped by Ce ions, and another fraction $f_{F_2^-\to K}$ of the F_2^- centres are lost by non-radiative e–h recombination mechanisms.

$$f_{F_2^-\to STE} + f_{F_2^-\to Ce} + f_{F_2^-\to K} = 1, \tag{2}$$

where the fractions $f_{F_2^-\to STE}$, $f_{F_2^-\to Ce}$ and $f_{F_2^-\to K}$ are both temperature and Ce-concentration dependent.

Eq. (3) gives the relation between the three STE-decay possibilities. $f_{STE\to\nu}$ represents the fraction of STEs which decay radiatively. Another fraction of the STEs $f_{STE\to Ce}$ can transfer their energy to Ce^{3+} ions either via transfer processes of the Förster–Dexter type (which is temperature independent) or via trapping of the mobile STE by a Ce^{3+} ion (a process which is temperature dependent). Energy transfer between STEs and Ce centres is possible because of the overlap of STE emission and Ce^{3+} optical absorption bands, see Fig. 1. Also a fraction $f_{STE\to\Omega}$ can be thermally quenched.

$$f_{STE\to\nu} + f_{STE\to Ce} + f_{STE\to\Omega} = 1, \tag{3}$$

where the fractions $f_{STE\to\nu}$, $f_{STE\to Ce}$ and $f_{STE\to\Omega}$ are both temperature and Ce-concentration dependent.

Using Eqs. (1)–(3), expressions for the photon yields due to STE emission, $N_{STE\to\nu}$, and Ce luminescence, $N_{Ce\to\nu}$, can be derived, see Eqs. (4) and (5), respectively.

$$N_{STE\to\nu} = N_{eh}\, f_{h\to F_2^-}\, f_{F_2^-\to STE}\, f_{STE\to\nu}, \tag{4}$$

$$N_{Ce\to\nu} = N_{eh}\,(f_{h\to Ce} + f_{h\to F_2^-} f_{F_2^-\to Ce} + f_{h\to F_2^-} f_{F_2^-\to STE}\, f_{STE\to Ce}). \tag{5}$$

Taking into account the influence of temperature on the different interactions appearing in Eqs. (4) and (5), two sub-cases can be examined in more detail.

Between T ~100 and 160 K:

From previous studies on pure $LiYF_4$ and Er^{3+} or Pr^{3+}-doped $LiYF_4$, see [1, 2], it is known that F_2^- centres are immobile below $T \sim 160$ K. Consequently, the fractions $f_{F_2^-\to Ce}$ and $f_{F_2^-\to K}$ are both equal to zero and each F_2^- centre forms an STE, $f_{F_2^-\to STE} = 1$, see Eq. (2). Therefore, between $T \sim 100$ and 160 K, the photon yields due to STE emission and Ce-luminescence are given by the following expressions,

$$N_{STE\to\nu} = N_{eh} f_{h\to F_2^-} f_{STE\to\nu}, \tag{6}$$

$$N_{Ce\to\nu} = N_{eh}(f_{h\to Ce} + f_{h\to F_2^-} f_{STE\to Ce}). \tag{7}$$

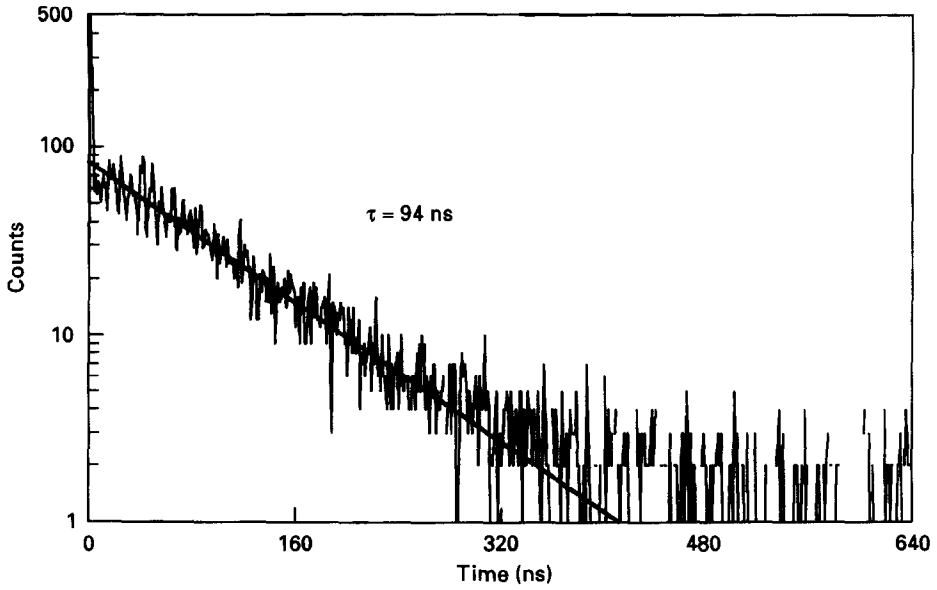

Fig. 4. Decay time spectrum of $LiYF_4$: 0.1 mol%Ce recorded with a ^{137}Cs source.

As the temperature is raised from $T \sim 108$ to 160 K, thermal quenching becomes the dominant decay process for STEs. Consequently, in Eq. (3), the fraction $f_{STE \to \Omega}$ increases up to 1 as the temperature is raised and both fractions $f_{STE \to v}$ and $f_{STE \to Ce}$ tend to zero. As can be seen from Fig. 3, the photon yield due to STE emission tends to zero while that due to Ce-luminescence reaches, for a given Ce-luminescence, a constant value given by $N_{eh} f_{h \to Ce}$.

Between T~160 and 380 K:
The F_2^- centres are now mobile. Their probability of being trapped at Ce or to decay non-radiatively, before STEs are created, increases with their mobility and hence with temperature. The photon yield due to STE emission, $N_{STE \to v}$, remains equal to zero. Apparently, between $T \sim 180$ and 250 K, the dominant contribution in the photon yield due to Ce-luminescence is caused by the direct transfer from the holes to Ce-centres, $N_{Ce \to v} = N_{eh} f_{h \to Ce}$. As the temperature is raised to ~ 380 K, the fraction $f_{F_2^- \to STE}$ decreases and consequently both fractions $f_{F_2^- \to Ce}$ and $f_{F_2^- \to K}$ are expected to increase. The photon yield due to Ce-luminescence can be described by

$$N_{Ce \to v} = N_{eh}(f_{h \to Ce} + f_{h \to F_2^-} f_{F_2^- \to Ce}). \quad (8)$$

As can be seen from Fig. 3, the photon yield due to Ce-luminescence increases as the temperature is raised to ~ 380 K, and at still higher temperatures the model predicts a constant value when the transfer of F_2^- centres to Ce ions will be at its maximal value.

4. Summary and conclusions

The optical and scintillation properties of Ce^{3+} doped $LiYF_4$ and $LiLuF_4$ crystals were studied. Large photon yields both under X-ray and γ-ray excitation, and a fast decay time with a large fast to slow ratio are some of the main requirements for scintillation crystals. Unfortunately, none of the different $LiYF_4$: Ce and $LiLuF_4$: Ce crystals studied fulfill these requirements and therefore none are suitable to provide a good thermal neutron scintillation detector. However, if both the charge traps responsible for slow decay components and non-radiative e–h recombination mechanisms are of extrinsic origin, decay time and photon yield could be improved by growing samples exempt of these charge traps.

Acknowledgements

These investigations have been supported by the Netherlands Technology Foundation (STW) and the Human Capital and Mobility project "Search for new and better scintillators for radiation detection".

References

[1] W. Hayes, M. Yamaga, D.J. Robbins and B. Cockayne, J. Phys. C 13 (1980) L1011.
[2] G.M. Renfro, L.E. Halliburton, W.A. Sibley and R.F. Belt, J. Phys. C 13 (1980) 1941.
[3] K.H. Yang and J.A. DeLuca, Phys. Rev. B 17 (1978) 4246.
[4] D.J. Ehrlich, P.F. Moulton and R.M. Osgood, Jr, Opt. Lett. 4(6) (1979) 184.
[5] J. Andriessen, H. Merenga, C.M. Combes, P. Dorenbos and C.W.E. van Eijk, in: Proc. Int. Conf. Inorganic Scintillators and their Applications, Delft, Netherlands, 1995, Eds. P. Dorenbos and C.W.E. van Eijk (Delft University Press, Delft, 1996) 142.
[6] A.R. Spowart, J. Phys. D 16 (1983) 1819.
[7] C.M. Combes, P. Dorenbos, C.W.E van Eijk, C. Pedrini and J.Y. Gesland, in: Proc. Int. Conf. Inorganic Scintillators and their Applications, Delft, Netherlands, 1995, Eds. P. Dorenbos and C.W.E. van Eijk (Delft University Press, Delft, 1996) 396.
[8] L.E. Erickson, Springer Ser. Opt. Sci. 49 (1985); Laser Spectrosc. 7, 287.
[9] E. Sarantopoulou, A.C. Cefalas, M.A. Dubinskii, C.A. Nicolaides, R. Yu Abdulsabirov, S.L. Korableva, A.K. Naumov and V.V. Semashko, Opt. Lett. 19 (7) (1994) 499.
[10] L. Esterowitz, R. Allen, M. Kruer, F. Bartoli, L.S. Goldberg, H.P. Jenssen, A. Linz and V.O. Nicolai, J. Appl. Phys. 48 (2) (1977) 650.
[11] E. Sarantopoulou, A.C. Cefalas, M.A. Dubinskii, C.A. Nicolaides, R. Yu Abdulsabirov, S.L. Korableva, A.K. Naumov and V.V. Semashko, Optics Commun. 107 (1994) 104.
[12] H.S. Kiliaan, A. Meijerink and G. Blasse, J. Lumin. 35 (1986) 155.
[13] Oak Ridge, Nat. Lab. Rep. 3761 (1965) 63.
[14] Oak Ridge, Nat. Lab. Rep. 3761 (1965) 52.
[15] R.D. Shannon, Acta Crystallogr. A 32 (1976) 751.
[16] P. Dorenbos, J.T.M. de Haas, R. Visser, C.W.E. van Eijk and R.W. Hollander, IEEE Trans. on Nucl. Sci. 40 (4) (1993) 424.